Politecnico di Milano
Gaia Biasolo, Matteo Giuseppe Cigada, Federico D'Agostini

Lab 01: Double track vehicle model

29/09/2025

Abstract

This lab analyzes vehicle handling dynamics with a 7-DOF double-track model and Magic Formula tire modeling. Linear and non-linear steady-state behaviors and linear transient responses are studied through steering pad and sine sweep maneuvers. The study compares an understeering and an oversteering tire set, evaluating the impact of cornering stiffness and relaxation lengths on vehicle stability.

Contents

1. Introduction

The aim of this laboratory is at first to investigate the influence of different tire sets on vehicle dynamics, analyzing both linear steady state behavior and non-linear steady state behavior. Afterwards, the influence of some parameters on the vehicle linear transient behavior (understeering/oversteering tendencies) is analyzed.

1.1 Double track vehicle model

The model considered for this lab is a double track vehicle model. Specifically, this model has 7 dofs (3 dofs for car body motion and 4 dofs for wheels rotation).

The **inputs** for this model are:

- Steering angle
- Driving and braking torques
- Road adherence
- Aerodynamic forces

The **outputs** are:

- Car body acceleration
- Car body velocity
- Car body position
- Wheel speed
- Contact forces

The forces considered inside the model are load transfer in longitudinal and lateral direction, rolling resistance and aerodynamic forces. The contact forces are evaluated through the Magic Formula (combined slip and relaxation length are considered).

1.2 Magic formula

As previously mentioned, the Pacejka Magic Formula was used to evaluate the tire contact forces. The simplified formula is the following:

$$F_y = Dsin\{Catan[B\alpha - E[B\alpha - \text{atan}\,(B\alpha)]]\}$$

Equation 1

- The parameters inside this formula are defined as:
  - D: peak factor
  - C: asymptotic factor
  - B: stiffness factor

- E: curvature factor

Cornering stiffness

In particular, coefficient B is linked to a parameter that was frequently used in this lab that is the cornering stiffness: K_y. This quantity represents the tangent of the curve of the lateral force vs slip angle in the origin (the higher K_y, the steeper the curve). Specifically:

$$B = \frac{K_y}{CD}$$

$$K_y = F_z\left(p_{Ky1} + p_{Ky2}dF_z\right)e^{p_{Ky3}dF_z}$$

Equation 2

As shown by the second formula, the cornering stiffness is highly influenced by the vertical load in a nonlinear way.

In this report cornering stiffness will be used as a tuning parameter to obtain the desired vehicle behavior, because it is the most influential parameter in the linear range.

2. Linear steady-state behavior

Steering pad at constant speed

The maneuver considered in this section is a steady state, open loop maneuver:

- The speed is constant
- The steering wheel angle is linearly increased
- The radius of the trajectory is measured

Since the linear behavior of the vehicle is investigated in this section, the diagrams presented are cut to make sure that the non-linear part of the simulation is neglected. They have considered up to the point where the lateral acceleration $a_y < 0.4g$

At first an **understeering vehicle** is taken as a **reference,** and multiple simulations are performed at different speeds (2.1). Successively, the speed is fixed at 50 km/h and a comparison between the reference vehicle and an oversteering vehicle is performed (2.2). In the end, the tire parameters of the understeering vehicle are modified to achieve neutral behavior (2.3).

2.1 Different speed test

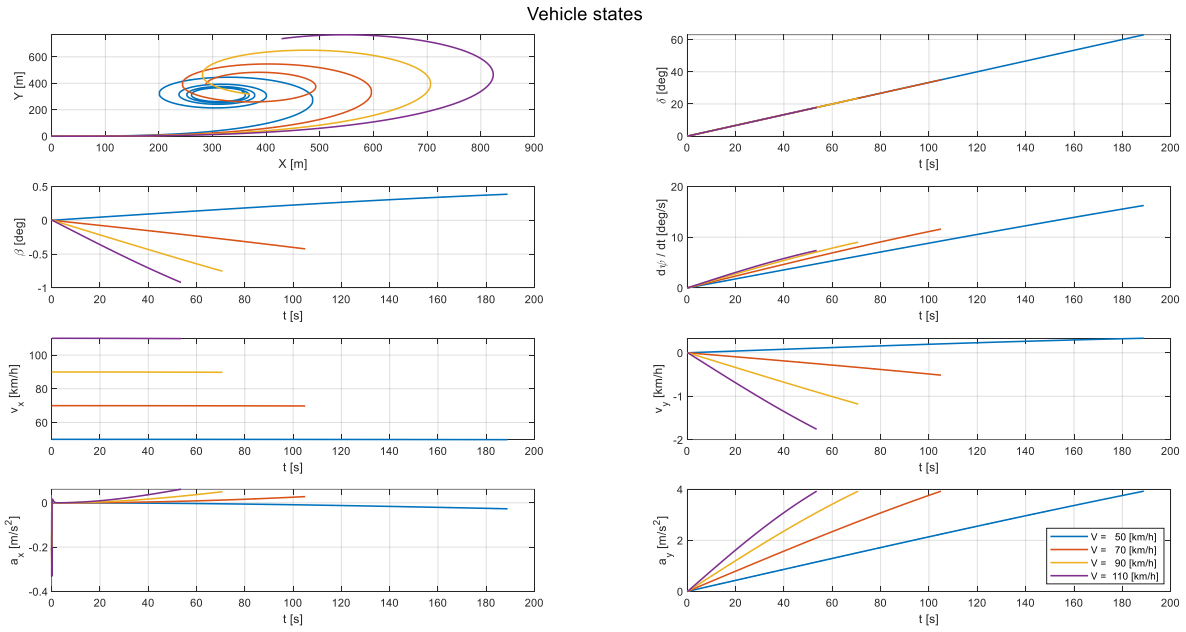

Figure 1

- the a_y, t diagram clearly shows where the linear region limit has been set as previously discussed

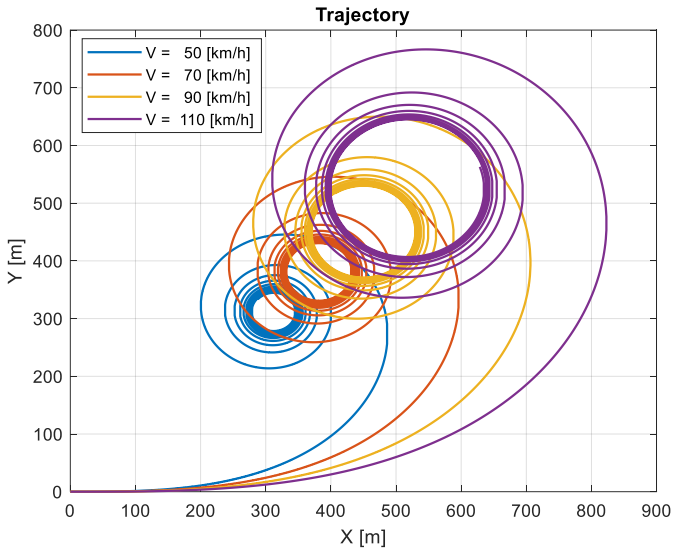

Figure 2

- The trajectory of the whole maneuvers (including the non-linear region) is displayed, clearly as the speed increases also the radius of the trajectory increases

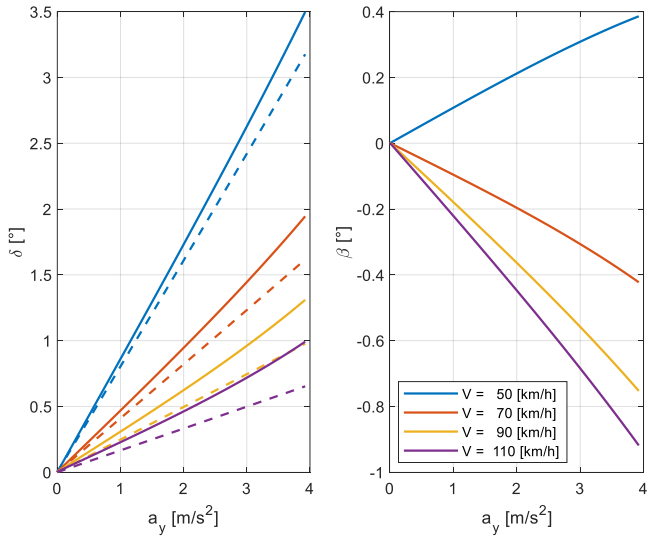

Figure 3

- The dashed lines represent the kinematic vehicle for each speed:

$$\delta_0 = \frac{l}{R} = \frac{l}{V^2} a_y$$

Equation 3

- The continuous lines on the other hand represent the behavior of the reference vehicle

- δ, a_y diagram:
  - The fact that the continuous lines always have a higher slope compared to the corresponding dashed lines simply indicates that the reference vehicle is indeed understeering:

$$\frac{\partial \delta}{\partial a_y} = \frac{l}{V^2} + K_{us} l \Longrightarrow \begin{cases} K_{us} > 0 \text{ (understeering)} \Leftrightarrow \text{slope higher than neutral} \\ K_{us} < 0 \text{ (oversteering)} \Leftrightarrow \text{slope lower than neutral} \end{cases}$$

Equation 4

- β, a_y diagram:
  - At low speed the side slip angle is positive → the velocity vector of the COM of the vehicle is pointing towards the inside of the turn (Figure 4)

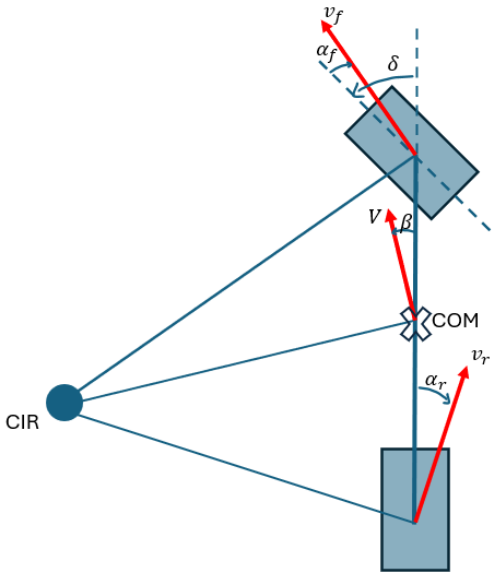

Figure 4

  - At higher speed the side slip angle is negative → the velocity vector of the COM of the vehicle is pointing towards the outside of the turn (Figure 5)

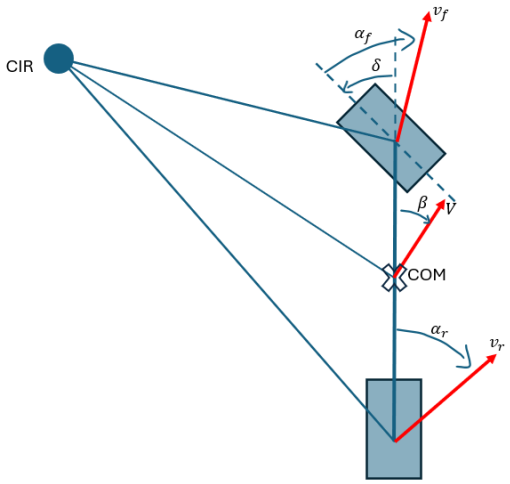

Figure 5

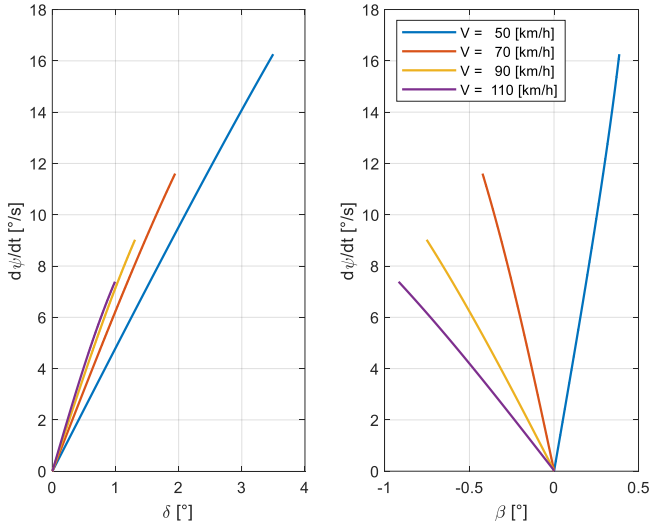

Figure 6

- From the single-track model equations, it can be derived that in steady state cornering the lateral acceleration can be written as $a_y = V\dot{\Psi}$. Therefore, both diagrams provide similar information to the ones in Figure 3, as one of the two axes is simply multiplied by the speed V.

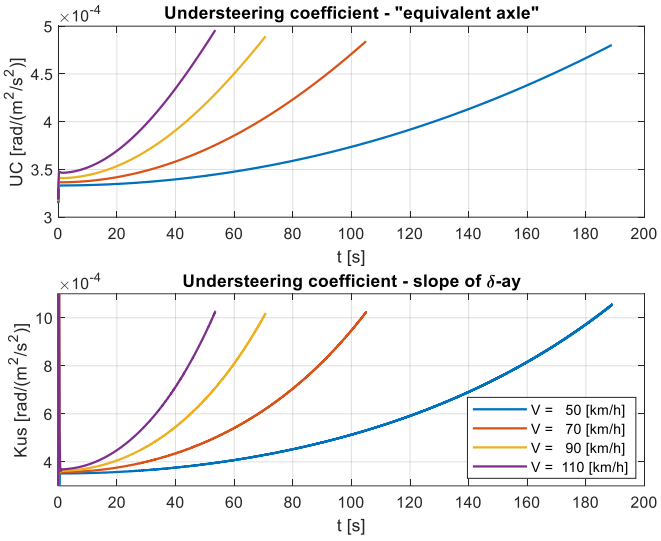

Figure 7

- The understeering coefficient is computed with two different approaches
  - **Top diagram: "equivalent axle approach"**
    - An "equivalent axle" cornering stiffness is computed:

$$\begin{cases} K_{y,front} = \text{mean}(K_{FL}, K_{FR}) * 2 \\ K_{y,rear} = \text{mean}(K_{RL}, K_{RR}) * 2 \end{cases}$$

Equation 5

    - The definition $K_{us} = \frac{m}{l^2}\left(\frac{l_r}{K_{y,front}} - \frac{l_f}{K_{y,rear}}\right)$ is used
  - **Bottom diagram "slope of δ, a_y"**
    - Equation 4 is used: the derivative is computed by making the point-by-point finite difference. This is causing numerical issues at the very first instant of the simulation where a spike is visible
- In any case, the understeering coefficient is always positive, thus the understeering behavior of the reference vehicle is confirmed once again

2.2 Different tires test

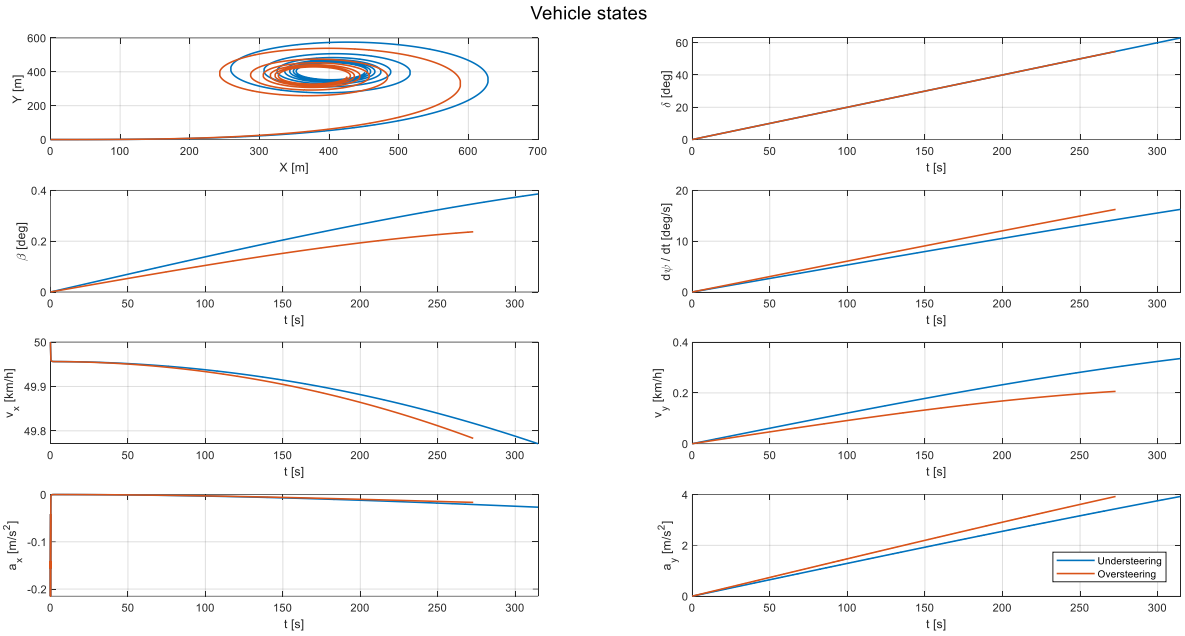

Figure 8

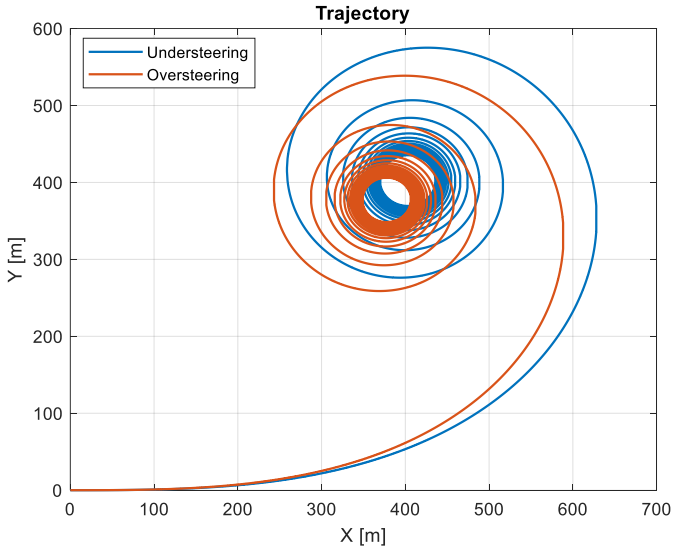

Figure 9

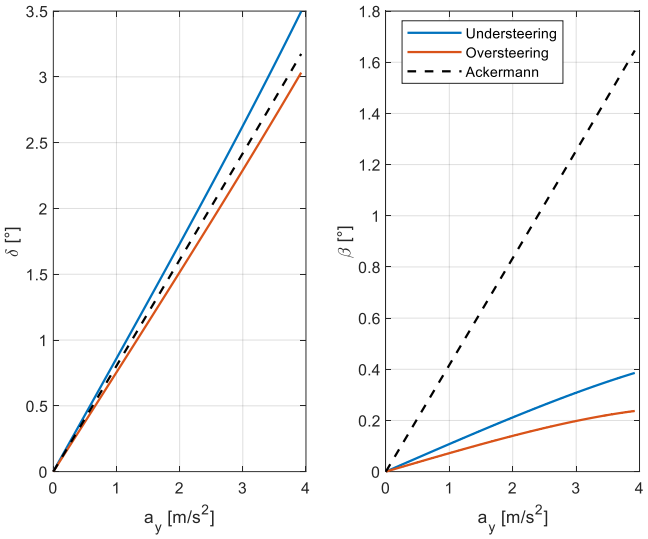

Figure 10

- Based on the considerations made in Equation 4:
  - The oversteering vehicle ($K_{us} < 0$) coherently has a δ, a_y curve with a slope lower than the line representing the kinematic vehicle
- The equation of the line representing the kinematic vehicle in the β, a_y plane is
  - $\beta = \frac{l_R}{V^2} a_y - \alpha_r$.

  The difference between the continuous lines and the dashed line is the rear slip angle
  - Coherently with the other diagram and with the theory, the oversteering vehicle has a higher rear slip angle compared to the understeering one

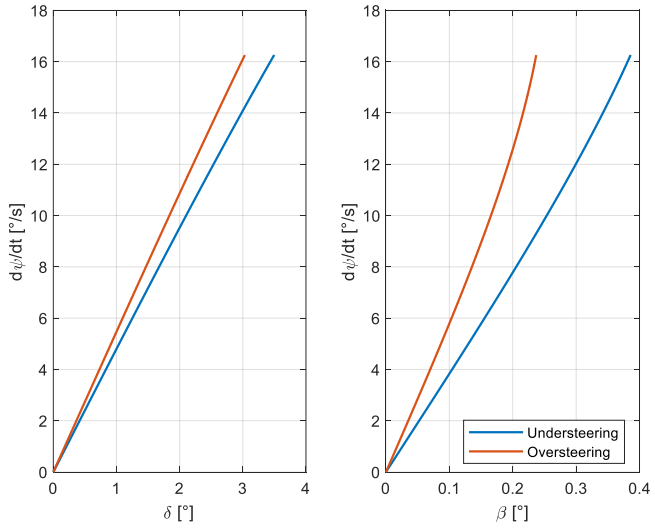

Figure 11

- Same considerations that hold for Figure 6.

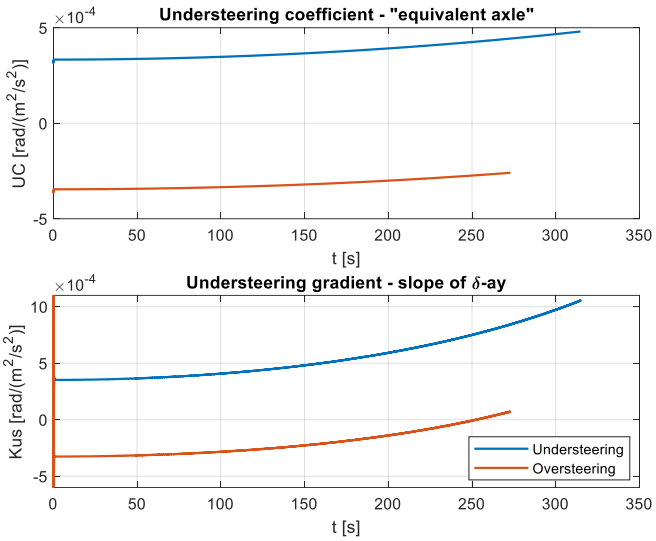

Figure 12

- As expected, the understeering coefficient for the oversteering vehicle is negative
    - Note that the bottom diagram suggests that at the end of the linear region Kus becomes slightly positive (understeering behavior), this in reality is coherent with the δ, a_y curve in Figure 10: the oversteering vehicle curve is almost parallel to the kinematic vehicle curve and at the very end it becomes slightly steeper. Even by looking at the trajectory (Figure 9) it seems like that the oversteering vehicle is showing an understeering behavior at the end of the maneuver.

2.3 Neutral car behavior

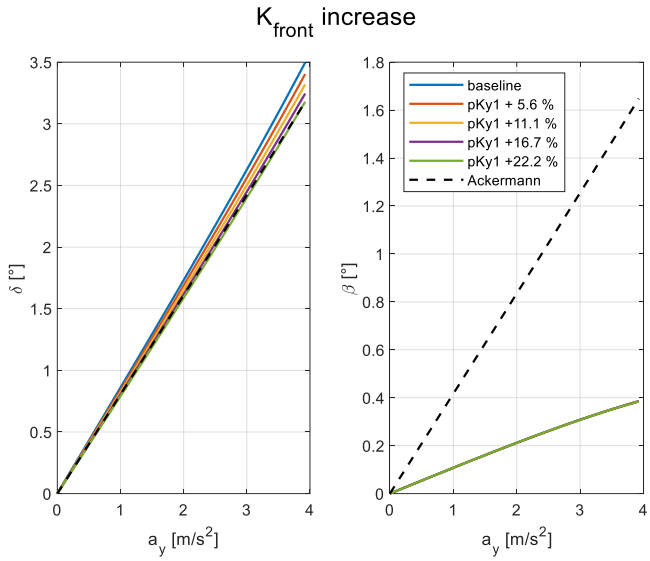

Figure 13

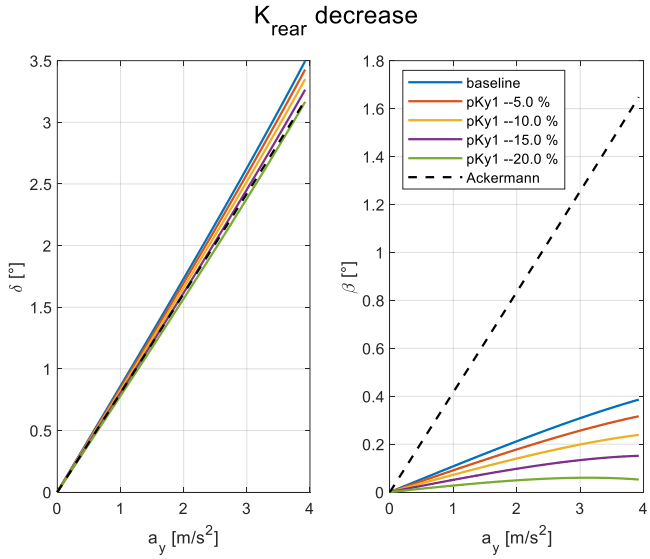

Figure 14

- By considering the F_y, α curve, two reasonable approaches can be adopted to change the behavior of a vehicle from understeering to neutral:
  - Increase the cornering stiffness at the front (Figure 13)
  - Decrease the cornering stiffness at the rear (Figure 14)
- In both cases, the δ, a_y diagrams indicate that the target is reached (the diagrams tend to become parallel to the neutral vehicle line)

- In the first case, the behavior of the β, a_y diagram does not change as K_{front} is increased; this is because the rear slip angle α_r is clearly not affected in any way by the cornering stiffness of the front axle
- In the second case on the other hand, the β, a_y diagram indicates that, as expected, the rear slip angle increases as K_{rear} decreases (for a fixed lateral force). Note that this doesn't mean that the vehicle becomes oversteering.

3. Non-linear steady-state behavior

Steering pad at constant speed

The maneuver considered in this section is identical to the one used in section 2.2, however, in this case, the nonlinear behavior of the vehicle is investigated. For this purpose, equivalent axle curves and handling diagrams have been used.

At first, a comparison between an understeering vehicle and an oversteering one is performed (3.2); successively, the tire parameters of both vehicles are modified to achieve a neutral behavior (3.3).

3.1.1 Computation of the handling diagram from experimental data

In this paragraph the computation of the handling diagram is necessary to evaluate the non-linear steady-state behavior of the vehicle.

In a handling diagram the difference between front and rear axle characteristics is plotted. The axle characteristics are defined as the normalized force of the axle plotted against the slip angle of the axle.

Therefore, the following data signals are considered:

- Slip angle at the front

$$\alpha_F = \delta - \tan^{-1}\left(\frac{v_y + \dot{\psi} * l_f}{v_x}\right)$$

- Slip angle at the rear

$$\alpha_R = -\tan^{-1}\left(\frac{v_y - \dot{\psi} * l_r}{v_x}\right)$$

- Normalized force at the front

$$F_F = \frac{F_{y_{FL}} + F_{y_{FR}}}{F_{z_{FL}} + F_{z_{FR}}}$$

- Normalized force at the rear

$$F_R = \frac{F_{y_{RL}} + F_{y_{RR}}}{F_{z_{RL}} + F_{z_{RR}}}$$

Finally, to compute the difference between the two curves, two final considerations are needed:

1. The handling diagram will be defined up to minimum between the two highest values of normalized force, one for each axle
2. Before the final difference is computed, since it is defined at constant normalized force, an interpolation of the array of slip angles on a common acceleration axis is performed.

3.2 Different tires test

Oversteering set

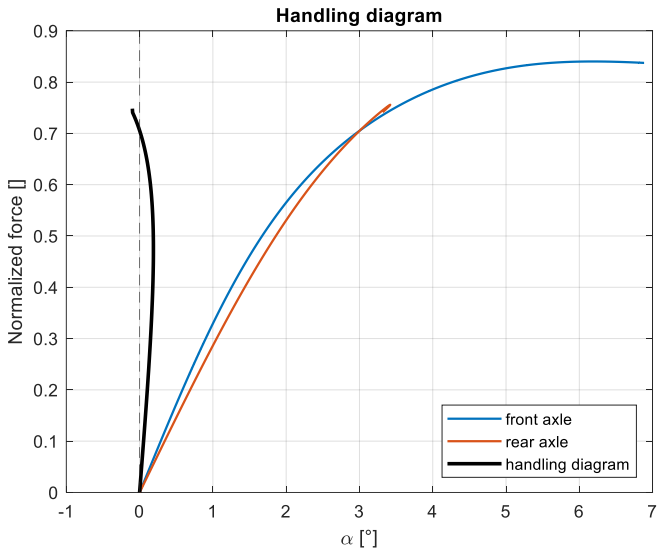

Figure 15

- The behavior is oversteering-understeering
    - In the first phase the car shows an oversteering behavior
    - At higher accelerations the car shows understeering behavior

Understeering set

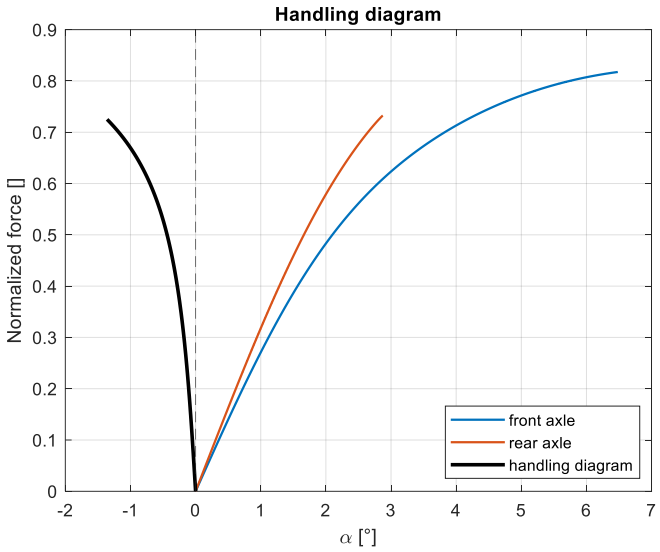

Figure 16

- The behavior is clearly understeering

3.3 Neutral car behavior

3.3.1 Oversteering tire set

Front cornering stiffness decreases

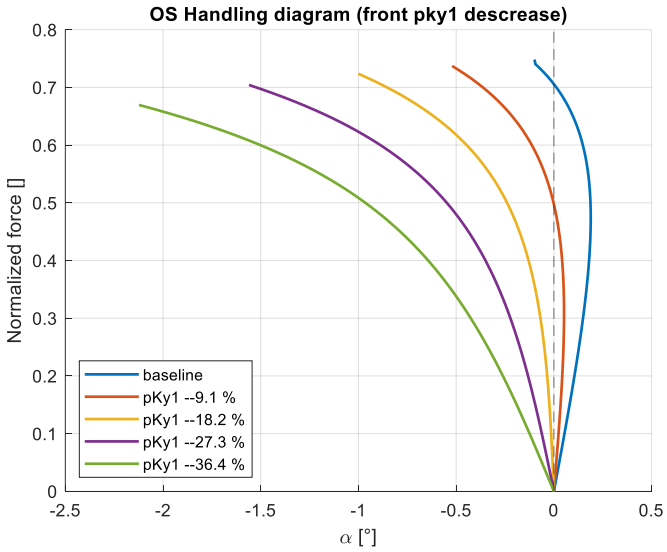

Figure 17

- The behavior of the vehicle shifts form oversteering to understeering. Which is coherent to the fact that to produce the same lateral force, a higher front slip angle is now needed
- The best presented option would probably be the pky1 reduction of 18.2%, which is the minimum reduction to make the car understeering and stable.

Rear cornering stiffness increases

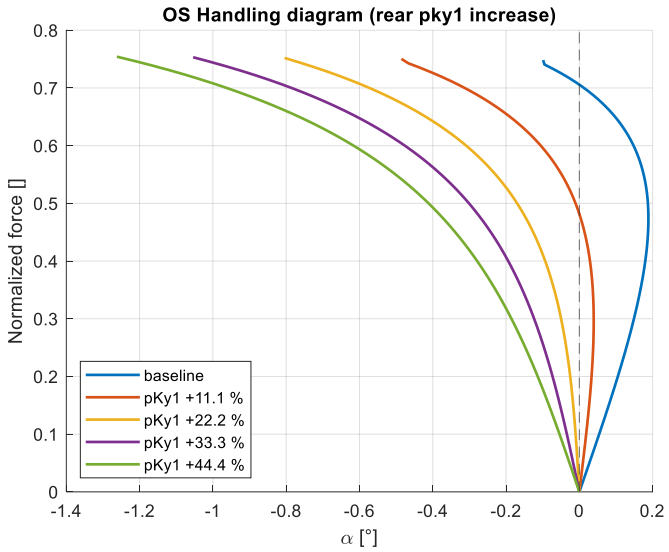

Figure 18

- The behavior of the vehicle shifts form oversteering to understeering. Which is coherent to the fact that to produce the same lateral force, a lower rear slip angle is now needed
- The best presented option would probably be the pky1 increase of 22.2%, which is the minimum increase to make the car understeering and stable.

3.3.2 Understeering tire set

Front cornering stiffness increases

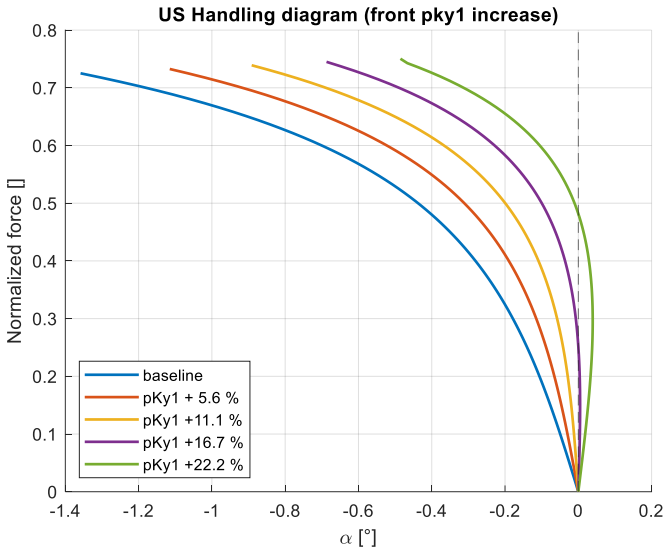

Figure 19

- The behavior of the vehicle shifts form understeering to oversteering. Which is coherent to the fact that to produce the same lateral force, a lower front slip angle is now needed
- The best presented option would probably be the pky1 increase of 16.7%, which is the maximum increase allowed not to make the car oversteering and unstable.

Rear cornering stiffness reduction

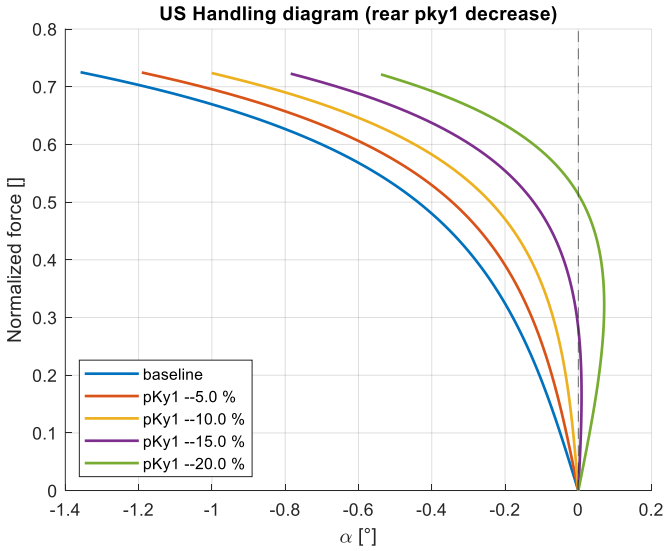

Figure 20

- The behavior of the vehicle shifts form understeering to oversteering. Which is coherent to the fact that to produce the same lateral force, a higher rear slip angle is now needed
- The best presented option would probably be the pky1 reduction of 10.0%, which is the maximum reduction allowed not to make the car oversteering and unstable.

For all the aforementioned options, for the same understeering or oversteering behavior, increasing the tires properties, regardless of the axle, reduces the vehicle slip angles for the same overall lateral acceleration.

4. Linear transient behavior

Steer sine sweep at constant speed

The maneuver considered in this section is a transient, open loop maneuver:

- The speed is constant
- The steering wheel angle is a sine function with progressively increasing frequency ($0\ \mathrm{Hz} \div 5\ \mathrm{Hz}$) and constant amplitude ($\pm 20°$)

At first, a comparison between an understeering vehicle and an oversteering one is performed (4.1); successively, the tire parameters of both vehicles are modified to achieve a neutral behavior (4.2).

4.1 Different tires test

Vehicle states understeering vehicle

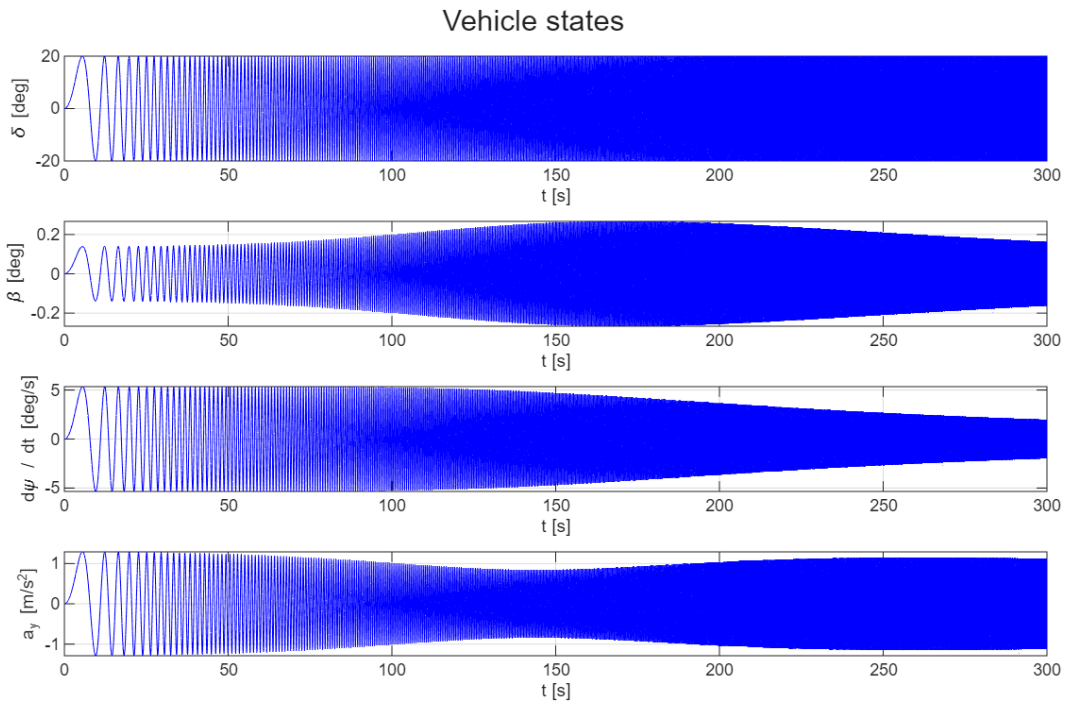

Figure 21

Vehicle states oversteering vehicle

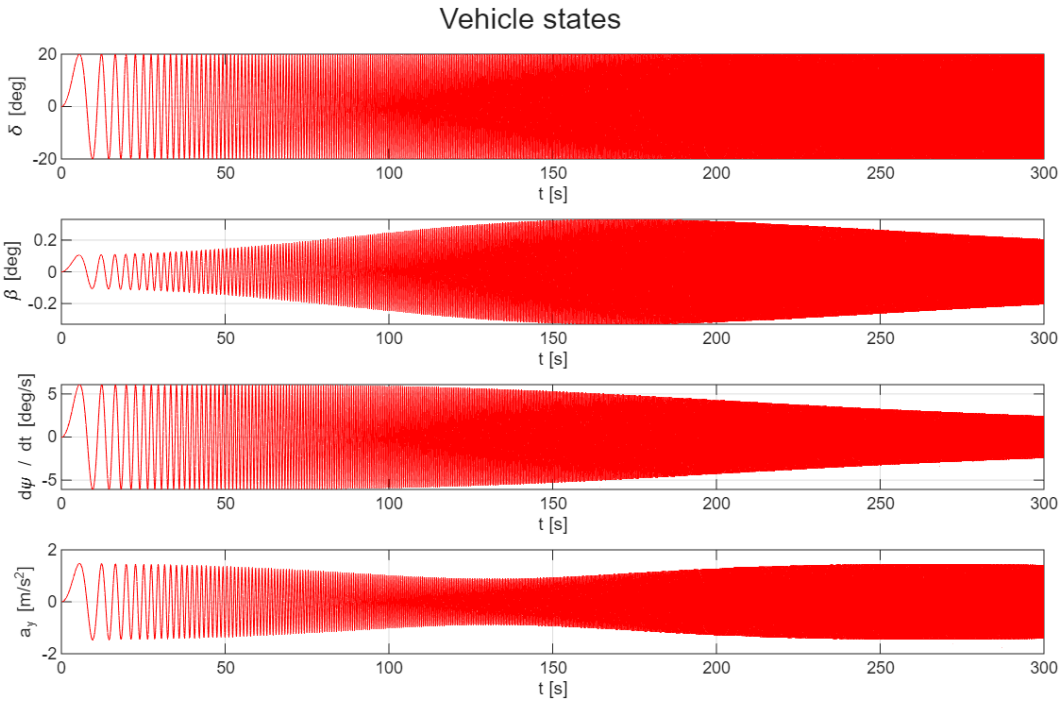

Figure 22

Vehicle states comparison

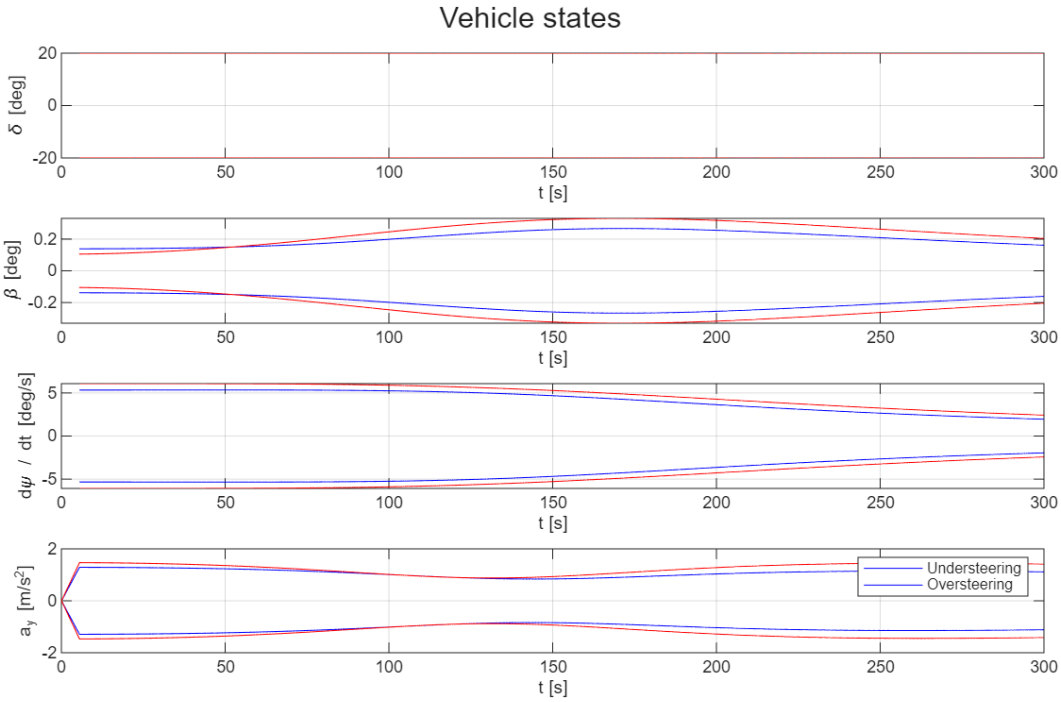

Figure 23

In Figure 21 the states of the vehicle with the **understeering** tire set are reported, while in figure Figure 22 the states of the vehicle with the **oversteering** tire set are presented. In Figure 23 a comparison between the maximum points of the two curves is plotted.

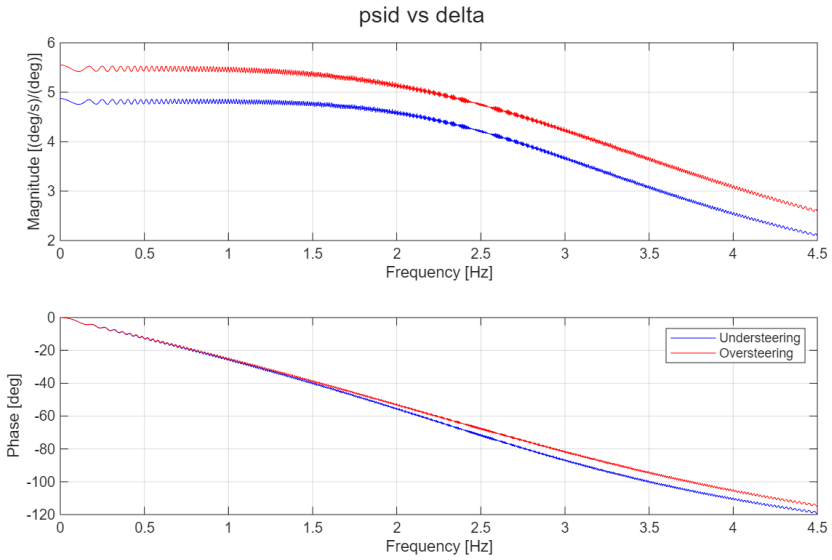

Figure 24

In Figure 24, the magnitude and the phase of the transfer function $\frac{\dot{\psi}}{\delta}$ are plotted. At low frequency, the response is flat for both sets of tires tend to be flat, implying linearity. The static gain of the oversteering set of tires is higher; this means that, imposing the same steering angle, the car will tend to rotate more around its axis. The understeering car tends to show a slightly higher phase lag at high frequencies, confirming a slower response. This results in a more stable but less agile vehicle.

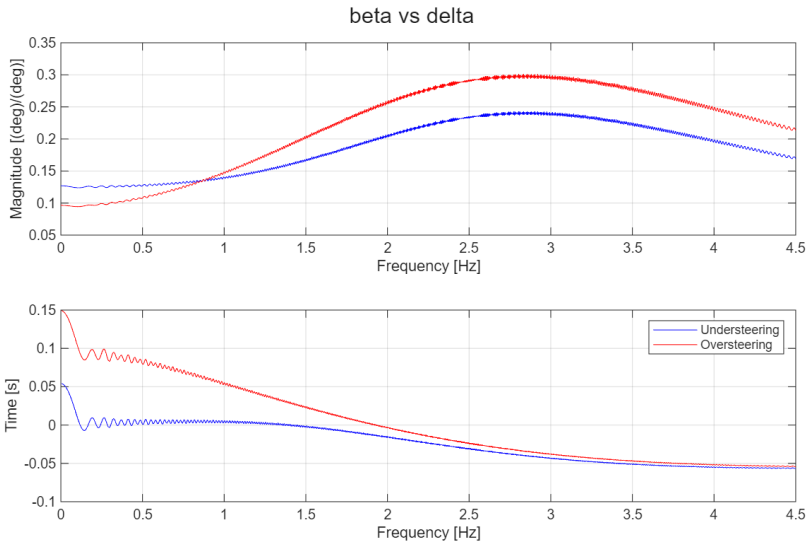

Figure 25

In Figure 25, the magnitude and the phase of the transfer function $\frac{\beta}{\delta}$ are plotted. The magnitude for both sets of tires shows a peak between 2 and 3 Hz, with the car with the oversteering set of tires showing the higher response. A higher beta gains indicates that the car tends to drift more when subject to fast steering inputs.

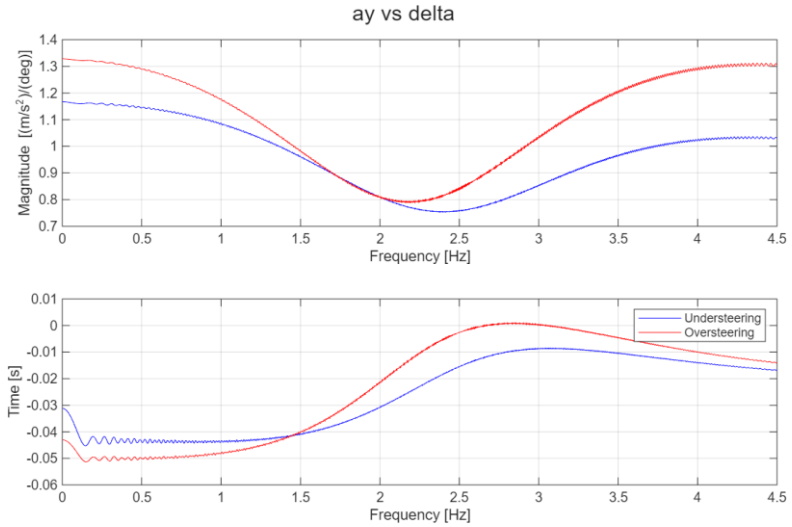

Figure 26

In Figure 26 , the magnitude and the phase of the transfer function $\frac{a_y}{\delta}$ are plotted. Once again, the oversteering set of tires generate a higher static gain meaning that the red car generates more lateral acceleration per degree of steering at low frequencies compared to the blue car. Moreover, both configurations show a minimum in the magnitude plot between 2 and 2.5 Hz: this reflects the system damping and the car with the understeering

set of tires, by showing a wider minimum implies lower efficiency in transferring commands to the ground during transients.

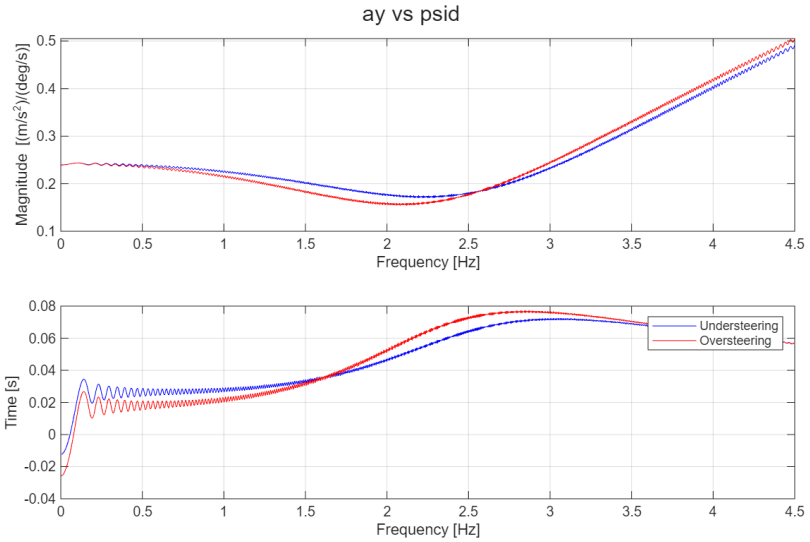

Figure 27

In Figure 27, the magnitude and the phase of the transfer function $\frac{a_y}{\dot{\psi}}$ are plotted. This is not a proper transfer function since it does not relate an input to an output but two outputs one to the other. This shows how the car's rotation translates into its actual path. The car with the oversteer set of tires shows more immediate rotation response, but the relationship with lateral acceleration differs from an understeering set, where the front slides before the car fully settles into the turn. The phase lag should be as small as possible especially at low frequency (around 1Hz) otherwise the vehicle would yaw without acceleration build-up (negative perception for the driver).

4.2 Neutral car behavior

The second request of the problem was to change the parameters of the understeering set of tires for it to have neutral behavior.

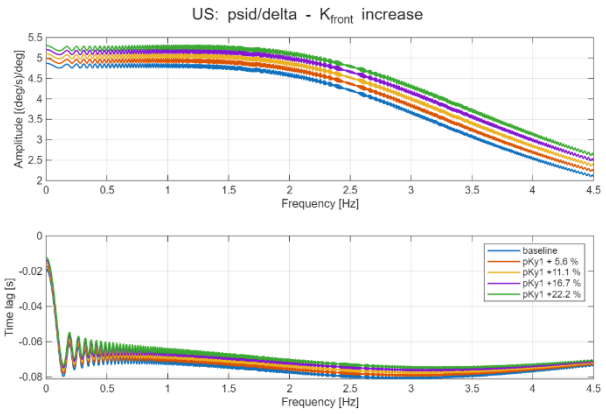

Figure 28

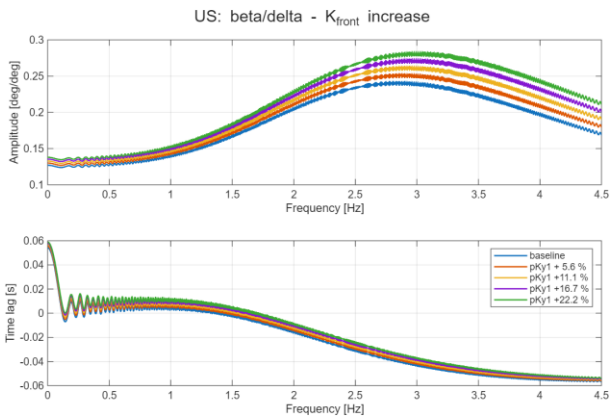

Figure 29

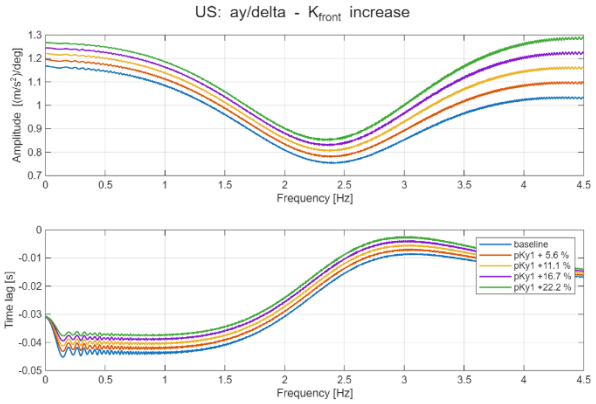

Figure 30

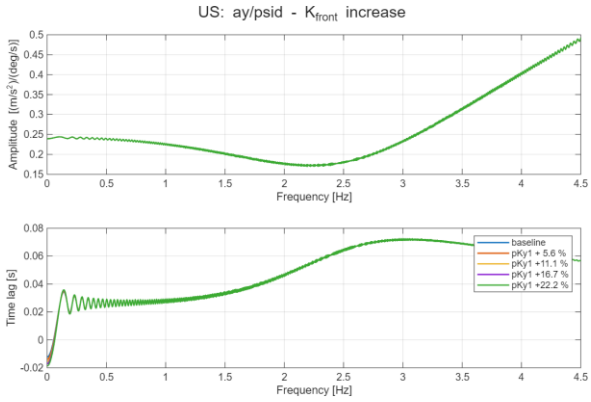

Figure 31

The first operation that was done to bring the understeering set of tires to a neutral one was to increase the front axle cornering stiffness. As it can be observed in Figure 28, Figure 29, and Figure 30, raising the stiffness increases the static gain: this means that given a certain steering input the car becomes more responsive as the front axle cornering stiffness increases. Moreover, it can also be noticed that the cut off frequency is reduced. This means that the car will be more responsive but for a shorter range of frequency.

Instead, by looking at Figure 31, it is evident that increasing the front axle cornering stiffness has no effect on the pseudo-transfer function linking the two outputs.

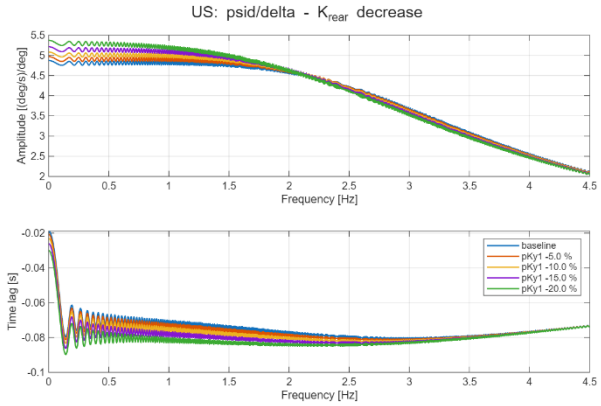

Figure 32

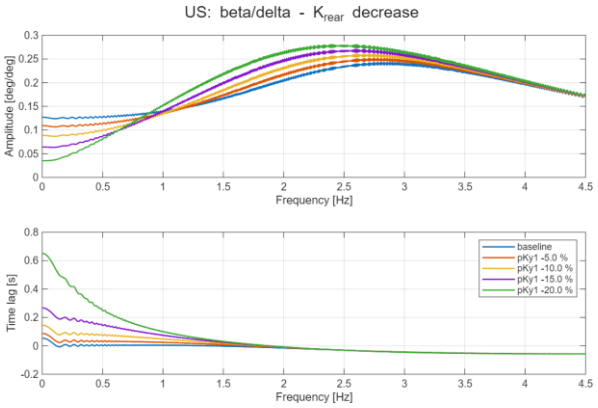

Figure 33

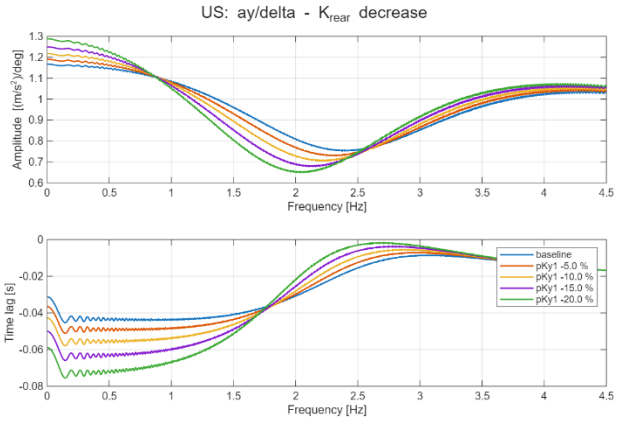

Figure 35

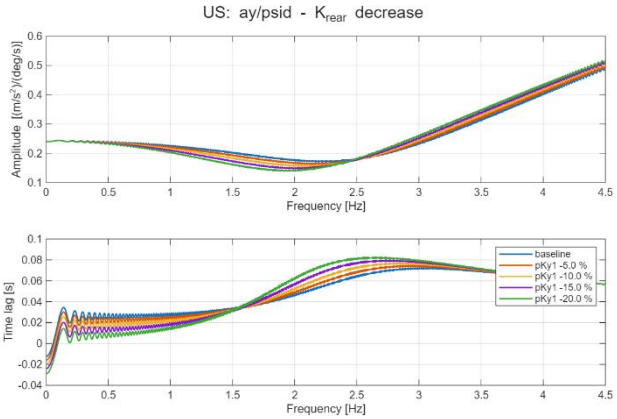

Figure 34

The second parameter that was varied to make the behavior of the car less understeering was the rear axle cornering stiffness, that needed to be decreased. This complementary operation allows the rear axle to generate higher slip angles that increases the yaw response and counteracts the original understeering tendency. From Figure 32, it can be appreciated that the vehicle now requires less steering input to achieve the same amount of rotation, at least at low frequency; this means that the response becomes sharper. In Figure 33, the most evident effect is that the time delay at low frequencies increases substantially as stiffness is reduced. The higher β peak and increased time lag indicate that the rear takes longer to settle and is more prone to oscillations during quick manoeuvres. In Figure 35, in the magnitude plot, the point of minimum gain becomes much more pronounced and shifts slightly toward lower frequencies. This suggests that in transient maneuvers lateral force buildup struggles.

5. Conclusion

The laboratory characterized the response of the double-track vehicle model across various operating conditions. In steady-state maneuvers, the understeering coefficient and handling diagrams provided a distinction between understeering and oversteering tire sets, confirming that cornering stiffness is the primary parameter influencing vehicle balance in the linear range. The transient analysis further demonstrated that while oversteering configurations offer higher yaw and acceleration gains, they also exhibit increased sideslip peaks, which can compromise stability during high-frequency inputs. Additionally, the study confirmed that neutral handling can be achieved by modifying some axle properties (such as increasing front stiffness or decreasing rear stiffness).